

# Understanding the Differences between Three Teleseismic $m_b$ Scales

by John P. Granville, Paul G. Richards, Won-Young Kim, and Lynn R. Sykes

**Abstract** We investigate differences between three body-wave magnitude ( $m_b$ ) scales for 2009 earthquakes from 1996 to 1999 listed in the Preliminary Determination of Epicenter (PDE) bulletin having  $m_b$  between 5.0 and 5.5 and that also have moment tensor solutions available from the Harvard Centroid Moment Tensor (CMT) catalog. A total of 31,280 broadband seismograms are analyzed, for an average of 15 stations per event. Both the PDE and Reviewed Event Bulletin (REB) procedures for determining an automated  $m_b$  are reproduced, thereby eliminating any discrepancies that result from using different networks of stations. We compare the reproduced PDE and REB magnitudes to another magnitude measurement,  $m_b(P)$ , that is based on the Worldwide Standard Seismographic Network (WWSSN) short-period instrument. We find that differences between  $m_b(P)$ ,  $m_b(\text{PDE})$ , and  $m_b(\text{REB})$  arise from four factors: response function, length of time window, and corrections for event depth and epicentral distance. Reproduced  $m_b(\text{PDE})$  and  $m_b(P)$  are strongly correlated, and we expect that magnitudes assigned from WWSSN short-period instruments during the 1970s and 1980s are consistent with those assigned by the automated procedure used since 1991 by the U.S. Geological Survey (USGS), providing stability in  $m_b$  measurements over several decades. The difference between  $m_b(\text{REB})$  and  $m_b(P)$  is much greater because of the significantly shorter REB window length of 5.5 sec and the high-frequency passband of the REB displacement response.

*Online Material:* Filter parameters and color versions of Figures 8 and 9.

## Introduction

The body-wave magnitude ( $m_b$ ) provides an empirical estimate of earthquake size that is directly related to the strength of ground shaking at teleseismic distances. Estimates of  $m_b$  are based on measurements of  $P$ -wave amplitude from short-period instruments (i.e., period  $\sim 1.0$  sec) and can be used to determine how strongly the ground moved at a specific location. Moreover,  $m_b$  can be used as a crude measure of seismically radiated energy, when direct estimates of radiated energy ( $E_s$ ) are not available (i.e., for earthquakes of  $m_b < \sim 5.5$ ). Nevertheless,  $m_b$  is increasingly regarded by some as a less important or less robust measurement of earthquake size since a more physically based measurement of earthquake size, the moment magnitude ( $M_w$ ), is now available for most moderate and large earthquakes. Yet,  $m_b$ , unlike  $M_w$ , is available for many events of  $m_b < 5$ . Furthermore, empirical  $m_b$  values have their own importance as a traditional measure of earthquake size assigned from short-period signals and are thus distinctly different from  $M_w$  values, which are estimated from long-period signals. Therefore, two events can have the same moment but a different  $m_b$ . For example, for two earthquakes of the same moment, one in a tectonically active region such as the western United States and one in a stable continental region such as eastern

North America, the event in the tectonically active region will be characterized by greater source-to-station attenuation. Consequently, the event in the stable region will typically have a higher  $m_b$  because of stronger ground shaking. Thus, assigning several types of magnitude (both empirical and physical) to an event allows for greater understanding of the earthquake source and the signals it generates.

This article focuses on teleseismic body-wave magnitudes assigned by the automated procedures of the United States Geological Survey (USGS) and the Prototype International Data Centre (PIDC). Significant discrepancies between short-period teleseismic magnitudes published by the USGS and PIDC were noted by Murphy and Barker (1996, 2003), Willemann (1998), Dewey (1999), and Murphy *et al.* (2001). These studies of body-wave magnitude discrepancies compared  $m_b$  values published by the two agencies in their respective bulletins of seismicity—the PIDC's Reviewed Event Bulletin (REB) and the USGS's Preliminary Determination of Epicenter (PDE) catalog. By analyzing only published values of magnitude (and the corresponding amplitude and period from which the magnitude is assigned), these studies were not able to address any bias in the actual amplitude and period measurements that results

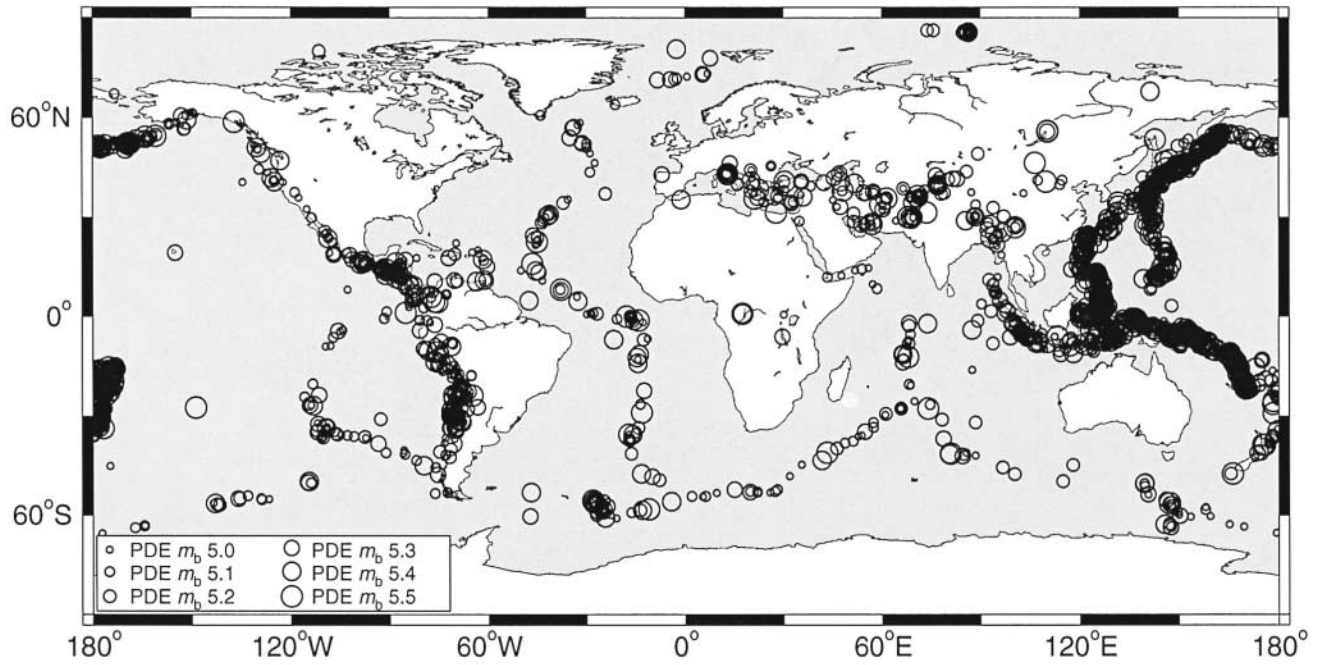


Figure 1. Locations of the 2009 earthquakes analyzed in this study (PDE bulletin  $m_b$  5.0–5.5). Symbol size increases with magnitude of PDE event.

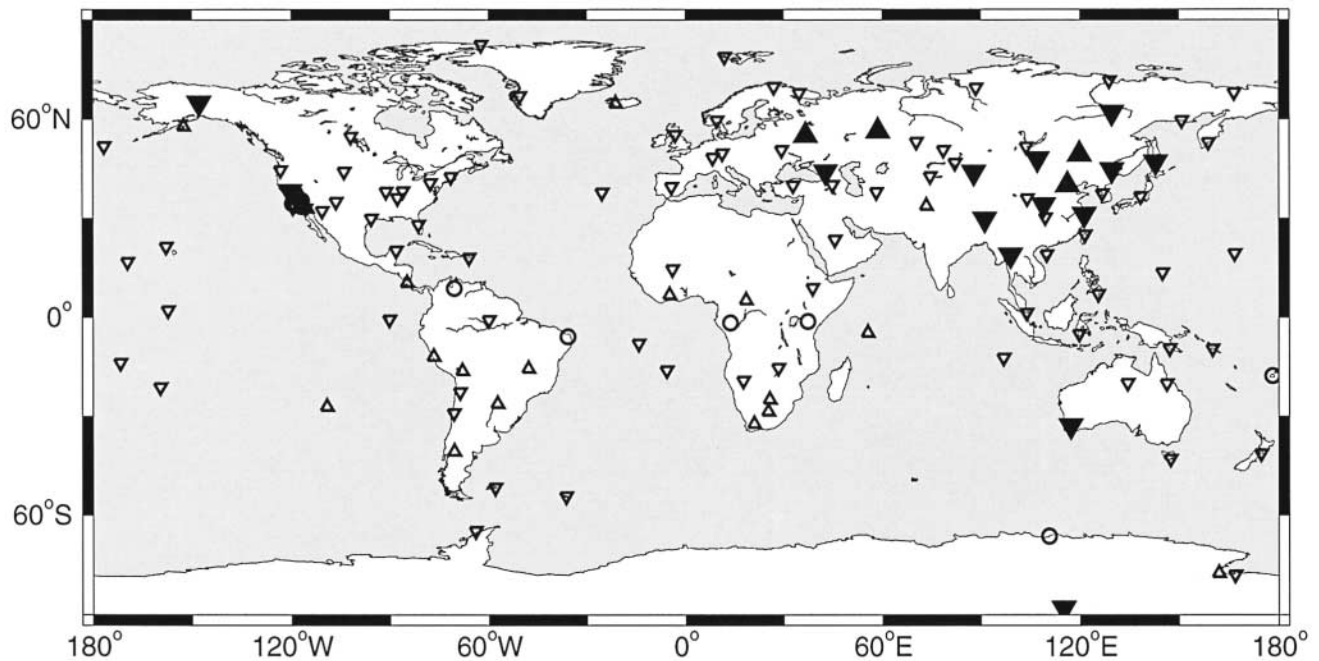


Figure 2. Locations of the 134 seismic stations used in this study. The 22 stations in our dataset that report data to both the USGS and PIDC are shown as triangles. There are 98 stations reporting only to the USGS and they are shown as inverted triangles (none of our stations report data only to PIDC). The remaining 14 stations in the dataset that do not report data to either the USGS or PIDC are shown as circles. Filled symbols indicate the 19 stations recording at least 25% of the earthquakes studied.

from the different filtering and time window lengths used by the different agencies and at various times. Moreover, these previous studies did not attempt to reproduce the magnitude procedures of either the USGS or PIDC.

Differences between published PDE and REB magnitudes result from different procedures for assigning magnitude as well as differences in the particular set of stations from which the magnitude is assigned. Only a small number of seismic stations are common to both the USGS and PIDC seismic networks. This problem of differing networks of stations is further complicated by the fact that many more seismic stations are available to the USGS for purposes of assigning magnitude than to the PIDC. Since the focus of this study is on differences in magnitude procedures and their effect on seismic magnitudes, we eliminate the problem of differing networks of stations by reproducing the automated protocols followed by the USGS and PIDC to assign  $m_b$ .

To understand these procedures used by the USGS and PIDC to assign  $m_b$ , we first describe exactly how these two agencies assign  $m_b$  from broadband, velocity waveforms and also how to reproduce their respective protocols and measurements. Since PIDC magnitudes were successfully reproduced by Granville *et al.* (2002), we follow their procedure to compute the PIDC magnitudes included in this study. The USGS procedure for assigning station  $m_b$  from broadband waveforms, on the other hand, has not been published and is not generally known. Guided by advice from USGS personnel (J. Dewey, personal comm., July 1998 to present), we are able to reproduce the automated procedure for assigning body-wave magnitude at USGS (i.e.,  $m_b(\text{PDE})$ ). Thus, we are confident that we understand how the USGS assigns magnitude, and we describe these procedures in detail in this article. We investigate differences between the USGS and PIDC magnitude scales, as well as a third magnitude scale,  $m_b(P)$ , that is based on a specific instrumental response—the Worldwide Standard Seismographic Network (WWSSN) short-period seismograph—that was widely used for over 20 years. We describe the differences between the three magnitude scales and then quantify the sources of the observed differences.

By duplicating the procedures of both the USGS and PIDC, we not only gain an understanding of exactly how magnitude measurements are made by these two agencies, but we also eliminate any discrepancies that arise from differing networks of stations. Our measurements are based on the same seismograms, allowing us to focus on the different protocols by which body-wave magnitudes are assigned. We find that differences between the three magnitude scales arise from four factors: response function, length of time window, corrections for event depth, and corrections for epicentral distance. The automated  $m_b$  procedure of the USGS is found to be a good surrogate for an  $m_b$  scale based on simulated WWSSN short-period instruments for the range of magnitudes studied (PDE bulletin  $m_b$  5.0–5.5 events). Magnitudes based on the automated PIDC procedure, on the other hand, are significantly smaller than those based on simulated

WWSSN short-period signals. Since the PIDC magnitude,  $m_b(\text{REB})$ , is a higher frequency measurement, it may perform better than a traditionally measured magnitude such as  $m_b(P)$  for purposes of applying the  $m_b$ – $M_s$  discriminant, although this has not yet been demonstrated. Further studies are necessary to determine whether the observed relationships between the three magnitude scales apply to events whose magnitudes are significantly different from those in this study.

For consistency with  $m_b(P)$  and  $m_b(\text{PDE})$ , the PIDC could produce a classical  $m_b$  measurement in addition to its current  $m_b(\text{REB})$ , styled after either the  $m_b(P)$  or  $m_b(\text{PDE})$  procedure. This classical measurement would be a very useful and important source parameter since it would be based upon a fixed network of stations and would be consistent with magnitudes measured using WWSSN short-period instruments.

## Method

### Data Acquisition and Processing

The dataset in this analysis consists of seismograms for 2009 earthquakes from 1996 to 1999 listed in the Preliminary Determination of Epicenter (PDE) bulletin having  $m_b$  between 5.0 and 5.5 and that also have moment tensor solutions available from the Harvard Centroid Moment Tensor (CMT) catalog (Fig. 1). In this dataset there are 463 earthquakes at PDE  $m_b$  5.0, 442 at PDE  $m_b$  5.1, 364 at PDE  $m_b$  5.2, 322 at PDE  $m_b$  5.3, 225 at PDE  $m_b$  5.4, and 193 events at PDE  $m_b$  5.5. Although the CMT catalog is not complete for earthquakes of PDE  $m_b$  5.0, the body-wave magnitude for which there are the most events in the CMT catalog nevertheless occurs at PDE  $m_b$  5.0. This suggests that a large subset of earthquakes of this size is characterized by sufficiently strong long-period signals to enable the computation of a moment tensor solution.

Our dataset consists of events with an associated PDE  $m_b$  between 5.0 and 5.5 because this range of magnitudes provides a representative global coverage (Fig. 1). Earthquakes with a PDE  $m_b$  less than 5.0 are omitted from this study because the azimuthal gap in station coverage is large and because there are often only a handful of nonarray stations for which data are available from the Incorporated Research Institutions for Seismology (IRIS) data center. We also exclude earthquakes with a PDE  $m_b$  greater than 5.5 because  $m_b$  begins to saturate above 5.5 and because there are fewer earthquakes at the larger magnitudes (Granville *et al.*, 2002, studied some of them). We chose a time period from 1996 to 1999 for our dataset because the only years for which a complete REB is publicly available are 1995 through 1999; however, in 1995, the first year that an REB was published regularly, the bulletin was plagued by problems such as incorrect instrumental responses and errors in the PIDC source code used to average the station  $m_b$  values (Granville *et al.*, 2002).

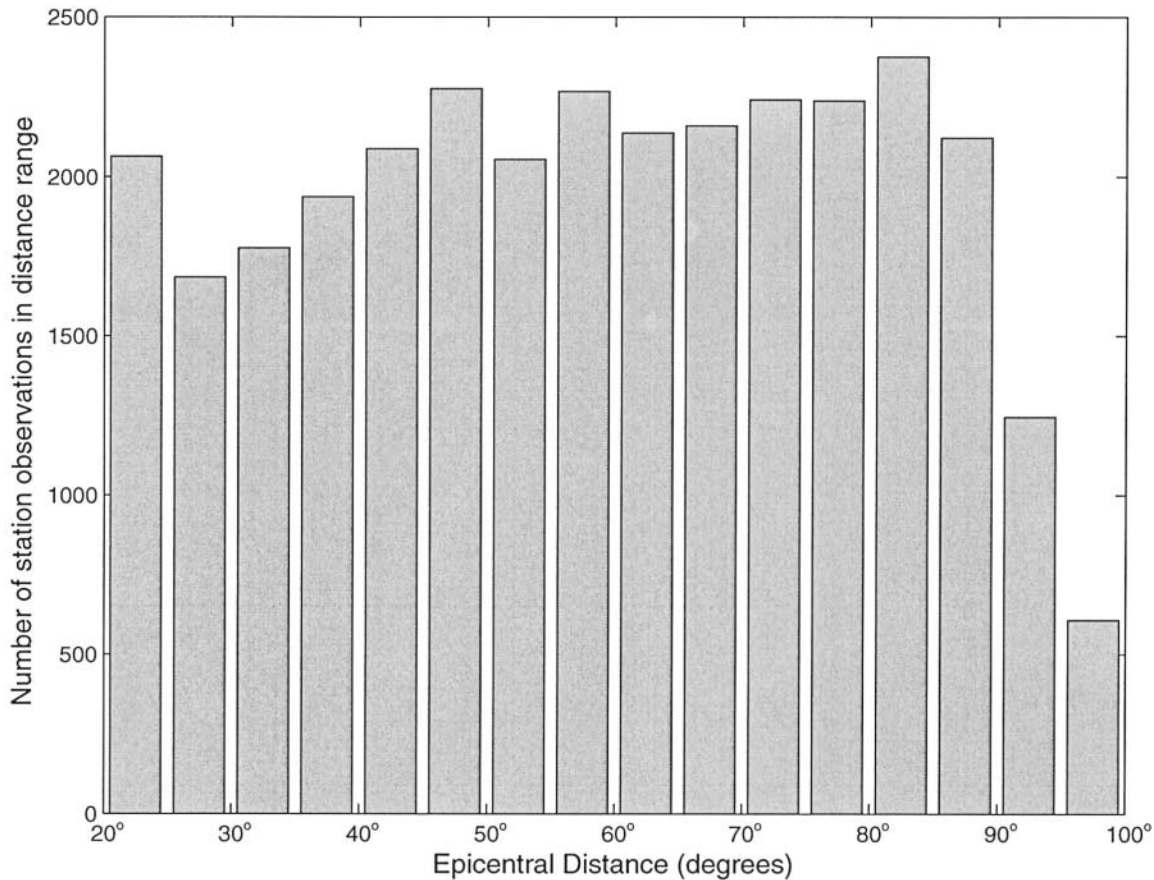


Figure 3. Histogram showing the number of stations recording an earthquake at different teleseismic distances, for all 31,280 individual station observations in this study. Each bin represents a range of distances with width 5°.

Data consist of broadband, vertical-component records for all Global Seismographic Network (GSN) stations between 20° and 100° from each of the earthquakes (i.e., the teleseismic distance range). Instrumental response information for all included stations was obtained with the waveform data. All data were obtained from the IRIS data center. A total of 134 seismic stations are used. In Figure 2, we show the locations of these stations and indicate which of them also reported data to the USGS and/or PIDC during 1996 to 1999. There are 22 stations in this study that reported data to both agencies. An additional 98 stations reported data only to the USGS. None of our stations reported data only to the PIDC. Finally, there are 14 stations in the dataset that did not report data to either the USGS or PIDC.

We find that 19 of the stations in this study recorded at least 25% of the events analyzed (Fig. 2). These 19 stations are predominantly located on the Eurasian continent, indicating that this region is the best location to record global earthquakes teleseismically. Moreover, only 2 of the 19 best-recording stations are in the southern hemisphere. Two of the stations in our study recorded more than half of the earthquakes in our dataset—WMQ in Urumqi, China (1177 events) and XAN in Xi'an, China (1224 events). The stations

included in this study provide good coverage over the entire teleseismic distance range (20°–100°). In Figure 3 we show the number of individual station observations in each teleseismic distance range using 5° bins. Only the farthest teleseismic distances (90°–100°) are not strongly represented, presumably because the Earth's core begins to have an effect on signal amplitude and reception.

All station body-wave magnitudes are calculated from filtered seismograms using the same general equation:

$$m_{b(sta)} = \log(A/T) + B(\Delta, h), \quad (1)$$

where  $sta$  is the station,  $A$  is the maximum half peak-to-trough amplitude in nanometers,  $T$  is the period in seconds measured at the maximum amplitude, and  $B$  is the correction for distance in degrees ( $\Delta$ ) and depth in kilometers ( $h$ ). A total of 31,280 broadband seismograms are included in this study, for an average of 15 stations per earthquake. Depth estimates are based on values from the Harvard CMT and USGS moment tensor catalogs. Since we expect the USGS moment tensor solution to provide the better estimate of hypocentral depth for shallow earthquakes, we preferentially include this depth where available (380 events total, the ma-

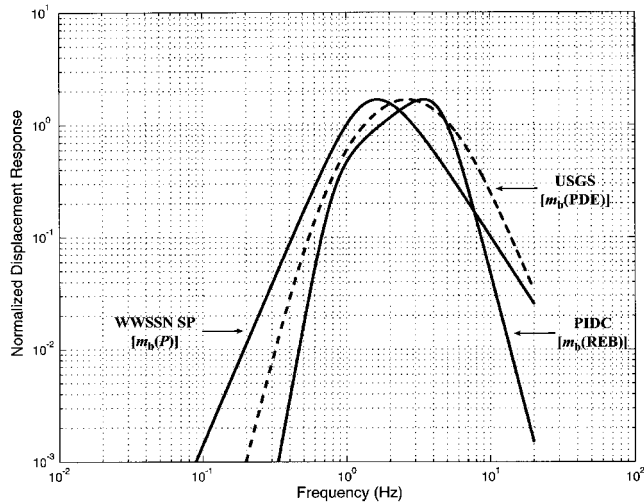


Figure 4. Displacement responses of a typical WWSSN short-period instrument, a broadband station processed according to the USGS procedure (bandpass filtering from 0.5 to 6.5 Hz and 1.05 to 2.65 Hz), and a broadband station processed according to the PIDC procedure (zero-phase bandpass filtered from 0.8 to 4.5 Hz). Responses are normalized to have the same peak gain.

majority of which correspond to our PDE  $m_b$  5.4 or 5.5 events). Otherwise, we calculate  $m_b$  using the depth from the Harvard CMT catalog. We use both the Veith–Clawson (1972) corrections for distance and depth as well as the Gutenberg–Richter (1956) corrections. Body-wave magnitudes computed using the Gutenberg–Richter correction are indicated as  $m_b^{\text{GR}}$ , while measurements that include the Veith–Clawson correction are given by  $m_b^{\text{VC}}$ . Although all body-wave magnitudes discussed in this study are computed using equation (1), differences arise between them because of different lengths of time windows, filters, response functions, and distance corrections.

Three types of body-wave magnitude are discussed in this article:  $m_b(P)$ ,  $m_b(\text{PDE})$ , and  $m_b(\text{REB})$ . The first,  $m_b(P)$ , is based on simulated WWSSN short-period signals and follows the procedure recommended by an International Association of Seismology and Physics of the Earth’s Interior (IASPEI) manual (Willmore, 1979). The second,  $m_b(\text{PDE})$ , is based on a reproduction of the automated procedure used since 1991 by the USGS to assign station magnitudes in its PDE bulletin. Finally,  $m_b(\text{REB})$  values are based on the automated procedure used by the PIDC to generate station magnitudes for its REB. We choose  $m_b(P)$  as our standard against which to compare PDE and REB  $m_b$  values because  $m_b(P)$  is a Richter-type magnitude (Richter, 1935) that follows a well-defined protocol and is based on a specific instrumental response—the WWSSN short-period seismograph—used for about two decades before broadband data became generally available. Neither the USGS nor PIDC magnitude scale is based on a particular instrumental response.

### $m_b(P)$ Procedure

To obtain a measurement of  $m_b(P)$  from the broadband  $P$ -wave recorded at a particular station, we first simulate a WWSSN short-period (SP) signal. This is done by deconvolving the response of the instrument to obtain ground displacement and then convolving the resulting waveform with the WWSSN SP displacement response (Luh, 1977). This short-period response is shown in Figure 4. Then, using the arrival times published in the International Seismological Centre (ISC) bulletin, the waveform is extracted for a 15-sec window beginning at the  $P$ -wave arrival time (referred to as either  $m_b(P)^{\text{GR},15\text{s}}$  or  $m_b(P)^{\text{VC},15\text{s}}$ , depending on the distance and depth corrections). The arrival times in the ISC bulletin are based on information contributed by several different agencies including the USGS and PIDC and are chosen for this study because the ISC reviews the contributed arrival times and selects the most accurate arrival time available for a given phase onset at a particular station. Measurements of  $m_b$  from the ISC bulletin are not included in this analysis because the ISC relies entirely upon contributed measurements of amplitude and period (including those published by the USGS and PIDC) instead of directly analyzing seismograms.

Amplitude and period are then measured from the simulated WWSSN SP waveforms in the 15-sec time window, and an  $m_b$  is assigned based on equation (1). Measurements of amplitude and period follow a traditionally used protocol described in the *Manual of Seismological Observatory Practice* (Willmore, 1979, p. 84), which states, “For earthquakes of small size, motions may be measured up to 20 seconds from the time of the first onset. For very large earthquakes, up to 60 seconds may be allowed.” Earlier guidelines gave a 15-sec window, followed here. The amplitude is measured from trough-to-peak (or peak-to-trough) and then halved to estimate the peak-to-zero ground motion in nanometers. Period is measured as peak-to-peak at the maximum amplitude. The quantity  $m_b(P)^{\text{VC},15\text{s}}$  is identical to the parameter referred to as Veith–Clawson  $m_b$  by Granville *et al.* (2002). The corresponding  $m_b(P)$  measurement that includes instead the Gutenberg–Richter distance and depth corrections is indicated as  $m_b(P)^{\text{GR},15\text{s}}$ .

### Reproduced $m_b(\text{PDE})$ Procedure

To assign  $m_b(\text{PDE})$  at a particular station, we follow an internal USGS memorandum that describes that agency’s automated procedure for measuring  $m_b$  (J. Dewey, personal comm., 1998). It is important to point out, however, that although we are able to reproduce the automated  $m_b$  procedure of the USGS, our  $m_b(\text{PDE})$  values may differ from the  $m_b$  values published by the USGS in its PDE bulletin for two reasons. First, a USGS analyst may override the automated procedure (for example, by following Willmore (1979) and selecting the maximum signal amplitude using a time window whose length exceeds the automated 10 cycle length and can be as long as 60 sec for very large earthquakes).

Second, the USGS publishes  $m_b$  values in its PDE bulletin that are contributed by other agencies. In fact, during the time period of our study (1996 to 1999) only  $\sim 30\%$ – $40\%$  of the amplitude ( $A$ ) and period ( $T$ ) measurements published in the PDE bulletin for  $m_b \geq 4.5$  earthquakes were measured internally by the USGS (J. Dewey, personal comm., 2003). The remainder of the ( $A$ ), ( $T$ ) measurements were contributed by agencies such as the Australian Geological Survey Organization, the Geological Survey of Canada, and the Laboratoire de Detection et de Geophysique, France. Although a significant number of station magnitudes published in the PDE bulletin are based on contributed values rather than the automated  $m_b$  procedure, we focus on the automated procedure because it is rigorously defined and can be accurately reproduced. The percentage of  $m_b$  measurements in the PDE bulletin that are based on the automated procedure has increased from around 15% in 1991 to about 45% in 2003 for  $m_b \geq 4.5$  events (J. Dewey, personal comm., 2004). Thus, there is an ongoing effort at USGS to standardize  $m_b$  measurements—that is, to base their measurements on an automated procedure.

We reproduce the automated procedure of the USGS by first demeaning the broadband, velocity record. Next, the signals are filtered using two bandpass filters: a second-order butterworth filter with cutoffs at 1.05 Hz and 2.65 Hz (2 zeros and 4 poles) and another second-order butterworth filter with cutoffs at 0.5 Hz and 6.5 Hz (2 zeros and 4 poles). The displacement response of these two bandpass filters is shown in Figure 4. (© The poles and zeros for these filters are given in Appendix 1, which is available in the electronic edition of BSSA.)

To measure amplitude and period, the filtered waveforms are then extracted for a 15-sec window beginning at the  $P$ -wave arrival, according to the ISC arrival time. Since the USGS uses a time window length of 10 cycles, beginning at the  $P$ -wave arrival, we obtain two slightly different measurements of maximum amplitude—one using a time window length of 15 sec (e.g.,  $m_b(\text{PDE})^{\text{GR},15\text{s}}$ ,  $m_b(\text{PDE})^{\text{VC},15\text{s}}$ ) and one using a length of 10 sec (e.g.,  $m_b(\text{PDE})^{\text{GR},10\text{s}}$ ,  $m_b(\text{PDE})^{\text{VC},10\text{s}}$ ). The measurement using a 15-sec time window is included to be consistent with  $m_b(P)$  while the magnitude measured in a 10-sec window is intended to approximate the time window used by the USGS (assuming a 1-sec period for 10 cycles). The amplitudes are measured from trough-to-peak (or peak-to-trough) and then halved to estimate the peak-to-zero amplitude. Periods are measured as peak-to-peak at the maximum amplitude.

The amplitudes are then corrected for the effect of the bandpass filtering and for instrumental response. The attenuating effect of the two bandpass filters is removed by dividing the measured amplitude by the amplitude of the filter response at the measured period (where the filter response consists of the combination of the two bandpass filters). This filter correction is quite large (a factor of 1.55 at 1 Hz) and is used to compensate for significant attenuation caused largely by the narrowband 1.05- to 2.65-Hz filter. The instrumental response (which is typically broadband and almost flat to velocity) is then removed by dividing the amplitude by the transfer function (to displacement) of the instrument at the measured period, providing an estimate of ground motion in nanometers. A body-wave magnitude is assigned for each of these amplitudes and their respective

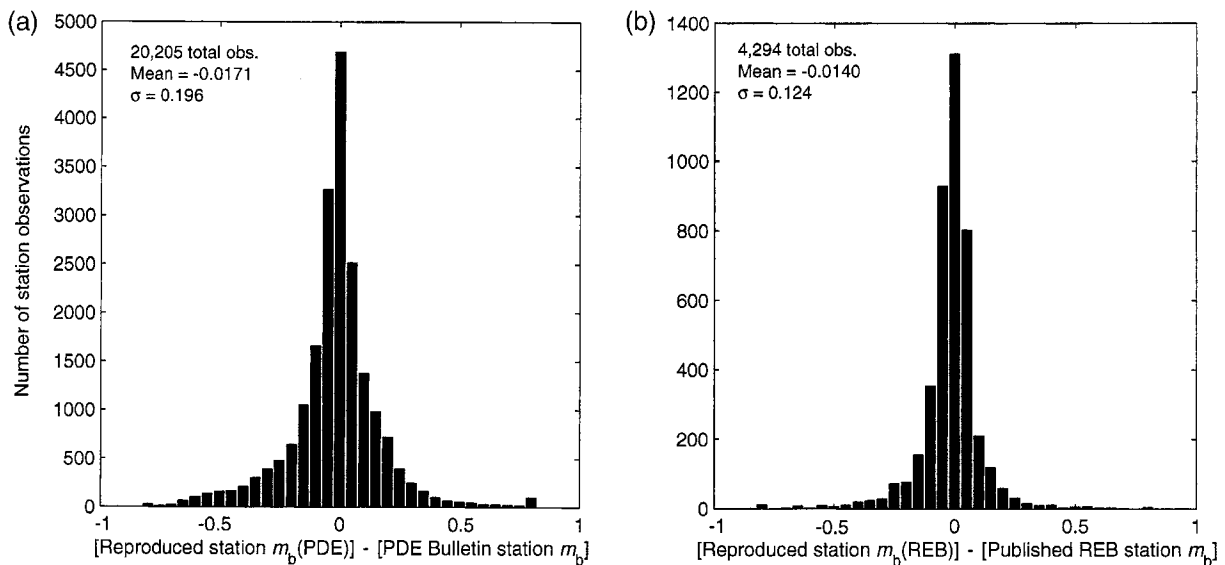


Figure 5. (a) Histogram showing the distribution of offsets between the reproduced PDE station  $m_b$  and the PDE bulletin station  $m_b$  for all earthquakes in the dataset (PDE bulletin  $m_b$  5.0–5.5). Each bin represents a range of offsets with width 0.05 magnitude units; (b) Histogram showing the distribution of offsets between the reproduced REB station  $m_b$  and the published REB station  $m_b$  for all events. Each bin represents a range of offsets with width 0.05 magnitude units.

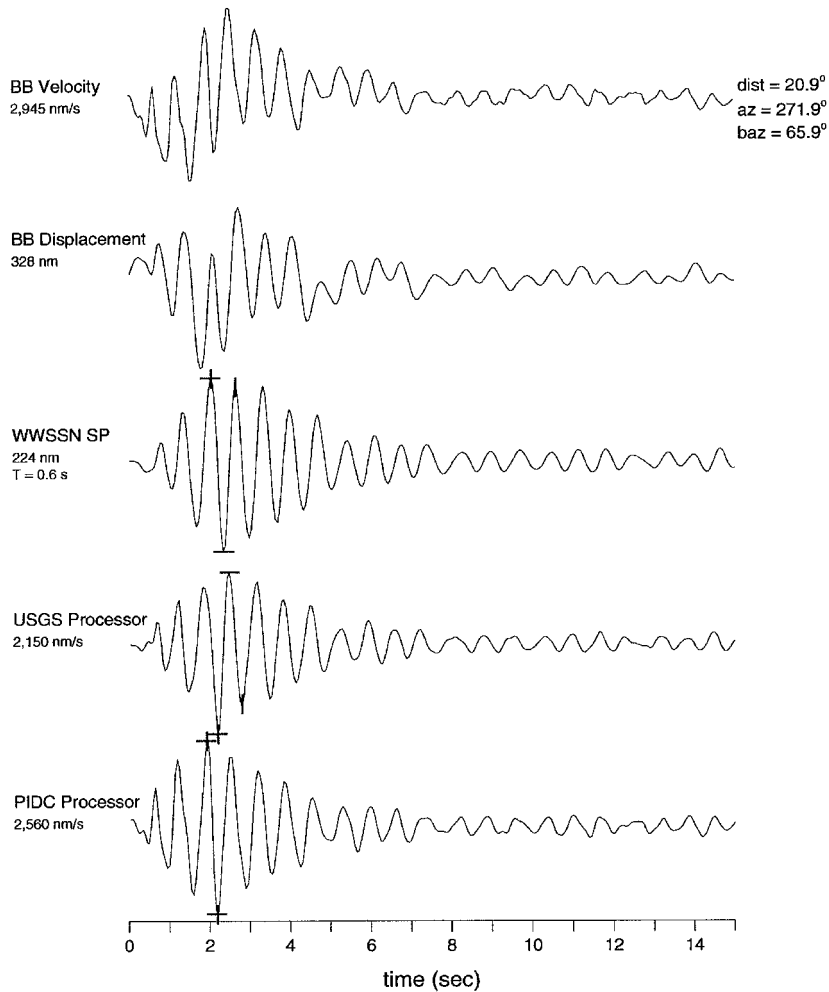


Figure 6. Simulated vertical records at HIA (Hailar, China) from the PDE  $m_b$  5.1 earthquake of 20 December 1997 in the Sea of Okhotsk region ( $h = 612$  km). Maximum amplitude (peak-to-trough or trough-to-peak) is marked by horizontal bars at the peak and trough of the measured amplitude and corresponding period is indicated by vertical bars. Note that for the USGS and WWSSN signals a full cycle period is measured whereas for the PIDC data a half cycle period is used. Maximum amplitude values, which are halved to estimate peak-to-zero (or zero-to-trough) amplitude, are given. For the simulated USGS short-period record, the corresponding displacement amplitude is 241 nm, with a period of 0.6 sec; the simulated PIDC short-period record has displacement amplitude of 204 nm, with a period of 0.5 sec. Waveforms begin at  $P$ -wave arrival time.

periods using equation (1). Since the USGS uses the Gutenberg–Richter corrections for distance and depth, the station magnitude corresponding to the  $m_b$  value published in the PDE bulletin is indicated by  $m_b(\text{PDE})^{\text{GR},10s}$ .

In Figure 5a we show the offset between our reproduced station  $m_b(\text{PDE})$  and PDE bulletin station  $m_b$  for the 20,205 observations that have an amplitude and period published in the PDE bulletin. The difference between the two magnitudes is  $-0.0171$  on average and the standard deviation ( $\sigma$ ) is 0.196. Agreement between the two quantities is not exact because, as previously stated, in many cases an analyst at the USGS will override the amplitude and period values assigned by the automated procedure and because many of the magnitudes published in the PDE bulletin are based on values contributed to the USGS by other seismological centers. The fact that our reproduced station  $m_b(\text{PDE})$  measurements are on average less than the corresponding values in the PDE bulletin is likely the result of analyst override at USGS. When overriding the automated measurements, an analyst may determine the maximum signal amplitude using a longer time window (up to 60 sec for large earthquakes) and therefore may assign a larger amplitude. Nevertheless, we are confident that our  $m_b(\text{PDE})$  accurately

reproduces the automated procedure stated by the USGS for assigning body-wave magnitude from a particular broadband record.

#### Reproduced $m_b(\text{REB})$ Procedure

The Reviewed Event Bulletin (REB) magnitude is reproduced by following the PIDC protocol for assigning  $m_b$  described in *IDC Processing of Seismic, Hydroacoustic, and Infrasonic Data* (International Data Centre, 1999) and is consistent with the method used by Granville *et al.* (2002) to reproduce magnitude values published in the REB. The REB magnitudes published by the PIDC are all measured using their automated procedure and there is minimal analyst override. It is important to point out, however, that although we are able to reproduce the automated  $m_b$  procedure of the PIDC, only 22 of the 134 stations in this study contributed data to the PIDC during 1996 to 1999. Therefore, our event magnitudes are based on a very different seismic network than those published by the PIDC.

To reproduce REB measurements, first the velocity signals are bandpass filtered using a third-order butterworth filter with cutoff frequencies at 0.8 Hz and 4.5 Hz. Since the

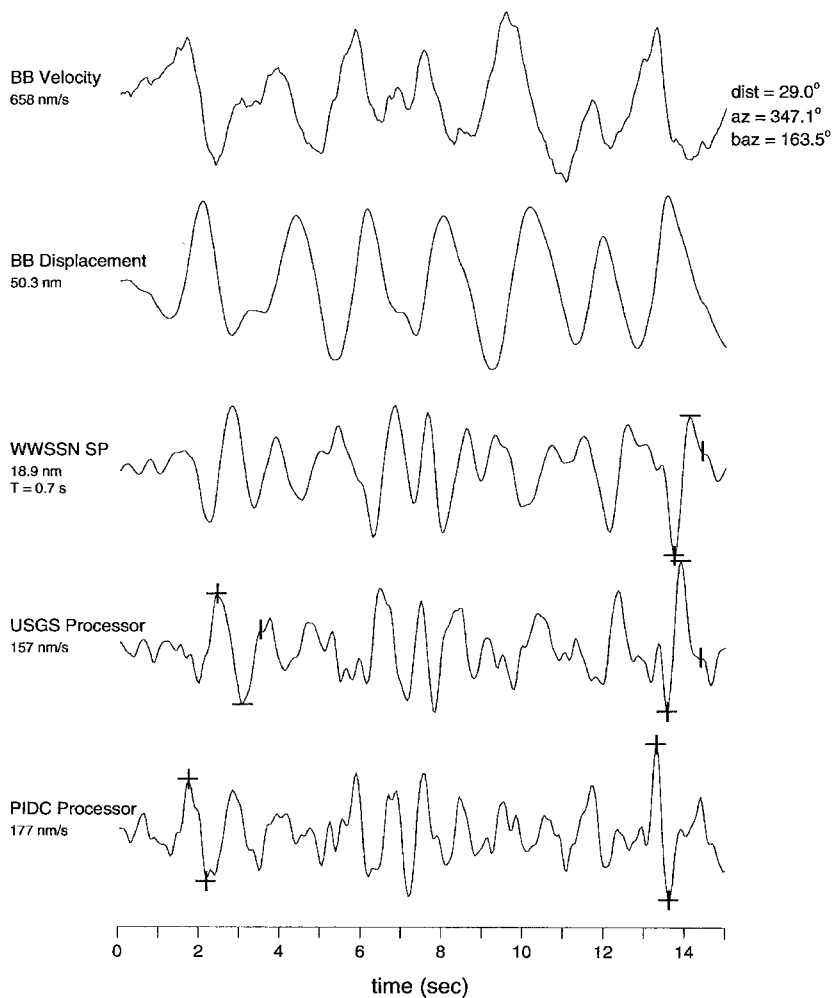


Figure 7. Simulated vertical records at BJT (Beijing, China) from the PDE  $m_b$  5.0 earthquake of 15 August 1999 in Leyte, Philippine Islands region ( $h = 34$  km). Maximum amplitude (peak-to-trough or trough-to-peak) is marked by horizontal bars at the peak and trough of the measured amplitude, and corresponding period is indicated by vertical bars. Note that for the USGS and WWSSN signals, a full-cycle period is measured, whereas for the PIDC data, a half-cycle period is used. Maximum amplitude values, which are halved to estimate peak-to-zero (or zero-to-trough) amplitude, are given. Since the maximum amplitudes for the reproduced USGS and PIDC waveforms arrive after the USGS- and PIDC-defined time windows (10 sec and 5.5 sec, respectively), we also indicate the maximum amplitudes that would be selected using the shorter time windows. For the simulated USGS short-period record, the corresponding displacement amplitude is 28.3 nm (with period of 1.0 sec) using a time window length of 10 sec and 27.4 nm (with period of 0.85 sec) using a 15-sec window. The simulated PIDC short-period signal has corresponding displacement amplitude of 16.5 nm (with period of 0.9 sec) using a time window length of 5.5 sec and 19.7 nm (with period of 0.7 sec) using a 15-sec window. Waveforms begin at  $P$ -wave arrival time.

PIDC uses a zero-phase, infinite impulse response (IIR) filter, the time series is then reversed in time and the data are filtered a second time, using the same bandpass filter. By filtering the data in both the forward and reverse directions, the waveform's shape is preserved, but the amplitudes are attenuated twice as much. The complete PIDC filter response thus consists of 12 poles and 6 zeros (each of the 6 unique pole values appears twice since the same filter is applied two times). The displacement response of these two bandpass filters is shown in Figure 4. (© The corresponding poles and zeros are given in Appendix 2, which is available in the electronic edition of BSSA.) The waveform is then extracted for a 15-sec window beginning at the  $P$ -wave arrival time. Then, we obtain two measurements of maximum amplitude from this waveform. The first amplitude measurement is measured using a 15-sec time window (e.g.,  $m_b(\text{REB})^{\text{GR},15\text{s}}$ ,  $m_b(\text{REB})^{\text{VC},15\text{s}}$ ), to be consistent with  $m_b(P)$ . The second is based on a window length of 5.5 sec (e.g.,  $m_b(\text{REB})^{\text{GR},5.5\text{s}}$ ,  $m_b(\text{REB})^{\text{VC},5.5\text{s}}$ ), to be consistent with the PIDC procedure for assigning  $m_b$ . The PIDC actually uses a time window length of 6.0 sec, beginning 0.5 sec before the  $P$ -wave arrival, however, we will refer to this time window length as 5.5 sec since this corresponds to the length of time after the  $P$ -wave

arrival. This nomenclature is consistent with measurements based on 10-sec and 15-sec time window lengths, since those window lengths are measured from the  $P$ -wave arrival time.

The amplitudes are measured as half trough-to-peak (or peak-to-trough). Periods are estimated as twice the time between the peak and trough corresponding to the measured amplitude. Then, the peak-to-zero amplitude is corrected for the instrumental response at the estimated period. The result is displacement amplitude in nanometers at the estimated period. Body-wave magnitude is assigned for each of the amplitudes and corresponding periods using equation (1). Since the PIDC uses Veith–Clawson corrections for distance and depth, the magnitude corresponding to the  $m_b$  published in the REB is indicated by  $m_b(\text{REB})^{\text{VC},5.5\text{s}}$ .

A comparison between our reproduced station  $m_b(\text{REB})$  and the published REB station  $m_b$  is shown in Figure 5B for the 4294 observations that have an amplitude and period published in the REB catalog. The difference between the two magnitudes is  $-0.0140$  on average, with  $\sigma = 0.124$ . Since the PIDC uses an automated procedure with minimal analyst override of measurements, we are able to match their measurements better than those of the USGS, where analyst override is more frequent. We do not include a correction

for the effect of the PIDC filter on the measured amplitudes, although the PIDC documentation does indicate that such a correction is applied (International Data Centre, 1999). In contrast to the large filter correction applied by the USGS, we expect this correction to be quite small—less than 10% on average. The frequency dependence of the PIDC displacement response in the 1 to 2 Hz frequency range of interest (Fig. 4) results almost entirely from the velocity-proportional instrument response.

## Results

### Individual Station Magnitudes

For each of the 31,280 broadband seismograms in this study, we measure the signal amplitude ( $A$ ) and period ( $T$ ) using five different automated procedures to generate five different measurements:  $m_b(P)$  from simulated WWSSN short-period signals,  $m_b(\text{PDE})$  using time window lengths of 10 sec and 15 sec, and  $m_b(\text{REB})$  using time windows of 5.5-sec and 15-sec duration. Moreover, for each of the five measurements of  $A$  and  $T$ , we compute an  $m_b$  using both the Veith–Clawson and Gutenberg–Richter distance and depth corrections; therefore, our results include 10 measurements of  $m_b$  per station for each event.

### Effect of Focal Depth on Seismograms

Examples of waveforms processed using these different procedures are shown in Figures 6 and 7. In Figure 6 we show the raw broadband signal as both velocity and displacement as well as the simulated WWSSN short-period record, the reproduced USGS short-period signal, and the reproduced PIDC short-period signal. The signals correspond to a deep ( $h = 612$  km) earthquake with PDE bulletin  $m_b$  5.1, as recorded by station HIA (Hailar, China). For this very deep earthquake, the simulated WWSSN, USGS, and PIDC waveforms are strongly correlated and the corresponding amplitude and period values are similar ( $A_{\text{WWSSN}} = 224$  nm,  $T_{\text{WWSSN}} = 0.6$  sec,  $A_{\text{USGS}} = 241$  nm,  $T_{\text{USGS}} = 0.6$  sec,  $A_{\text{PIDC}} = 204$  nm,  $T_{\text{PIDC}} = 0.5$  sec). The maximum amplitude for each of these three waveforms arrives within the first three seconds after the  $P$ -wave arrival, so the choice of time window is not an issue. The  $m_b^{\text{GR}}$  values associated with these records are nearly equal:  $m_b(P)^{\text{GR}} = 5.93$ ,  $m_b(\text{PDE})^{\text{GR}} = 5.96$ , and  $m_b(\text{REB})^{\text{GR}} = 5.96$ . Although the amplitude measured from the reproduced USGS short-period record in Figure 6 is smaller than the amplitude measured from reproduced PIDC short-period signal, the corresponding displacement amplitude for the simulated USGS signal is larger than the PIDC displacement amplitude because the USGS applies a large filter correction to their amplitude measurements. This filter correction is intended to compensate for the significant attenuation in signal amplitude that results from applying the two USGS bandpass filters.

For a shallow earthquake, on the other hand, the simulated WWSSN, USGS, and PIDC waveforms can appear quite

different (Fig. 7). We show the raw broadband signal (in both velocity and displacement) as well as the simulated WWSSN short-period record, the reproduced USGS short-period signal, and the reproduced PIDC short-period signal in Figure 7. The records correspond to a shallow ( $h = 34$  km) PDE earthquake of  $m_b$  5.0 recorded at station BJT (Beijing, China). For this shallow event, the maximum amplitudes arrive much later in the wavetrain than for a deep event. In this case, since the USGS and PIDC assign their magnitudes using time window lengths of less than 15 sec (10 sec and 5.5 sec, respectively), the amplitude that would be assigned by these agencies is smaller than the maximum amplitude within the full 15-sec window (Fig. 7). For the simulated USGS short-period waveform, the corresponding displacement amplitude is 28.3 nm (with a period of 1.0 sec) when measured in a window of length 10 sec and 27.4 nm (with a period of 0.85 sec) using a 15-sec window. The simulated PIDC waveform has displacement amplitude of 16.5 nm (with a period of 0.9 sec) when measured with a window of length 5.5 sec and 19.7 nm (with period of 0.7 sec) using a 15-sec window. The corresponding  $m_b(\text{PDE})^{\text{GR},10\text{s}} = 4.91$  and  $m_b(\text{PDE})^{\text{GR},15\text{s}} = 4.97$ ;  $m_b(\text{REB})^{\text{GR},5.5\text{s}} = 4.72$  and  $m_b(\text{REB})^{\text{GR},15\text{s}} = 4.91$ . The simulated WWSSN SP signal has  $m_b(P)^{\text{GR}} = 4.89$ . Since the USGS displacement amplitude has been corrected for the effect of two filters, this displacement amplitude is greater than the corresponding PIDC displacement amplitude (even though the opposite is true for the velocity amplitudes).

### Relationship between $m_b(P)$ , $m_b(\text{PDE})$ , and $m_b(\text{REB})$

One goal of this study is to investigate how well correlated the automated USGS magnitude scale is to one based on the WWSSN short-period instrumental response. In Figures 8a and 8b, we show the relationship between  $m_b(\text{PDE})$  and  $m_b(P)$  and find that the two measurements are strongly correlated over all depth ranges. (© Color versions of these figures that include results for all six subsets of earthquakes [PDE bulletin  $m_b$  5.0 to 5.5] are available in the electronic edition of BSSA.) We expect that the depth range where the choice of time window (either 5.5 sec, 10 sec, or 15 sec) will have the greatest effect on  $m_b$  is from 15 to 50 km. This is because the direct-arrival  $P$  phase is often much smaller in amplitude than the surface-reflected depth phases  $pP$  and  $sP$  for earthquakes occurring at those depths. The arrival of the  $P$ -wave amplitude will also be affected by differences in source complexity. Many larger earthquakes are characterized by slowly emerging  $P$ -wave amplitudes, and the maxima are significantly delayed with respect to initial  $P$ -wave arrival times.

Since many of the shallow earthquakes studied are assigned a default depth of 15 km in the Harvard CMT catalog and an exact depth is not available, we treat these events separately. The  $m_b(\text{PDE})$  shown in Figure 8a uses a time window length of 10 sec, similar to the PDE procedure; in contrast, the window length for  $m_b(\text{PDE})$  in Figure 8b is

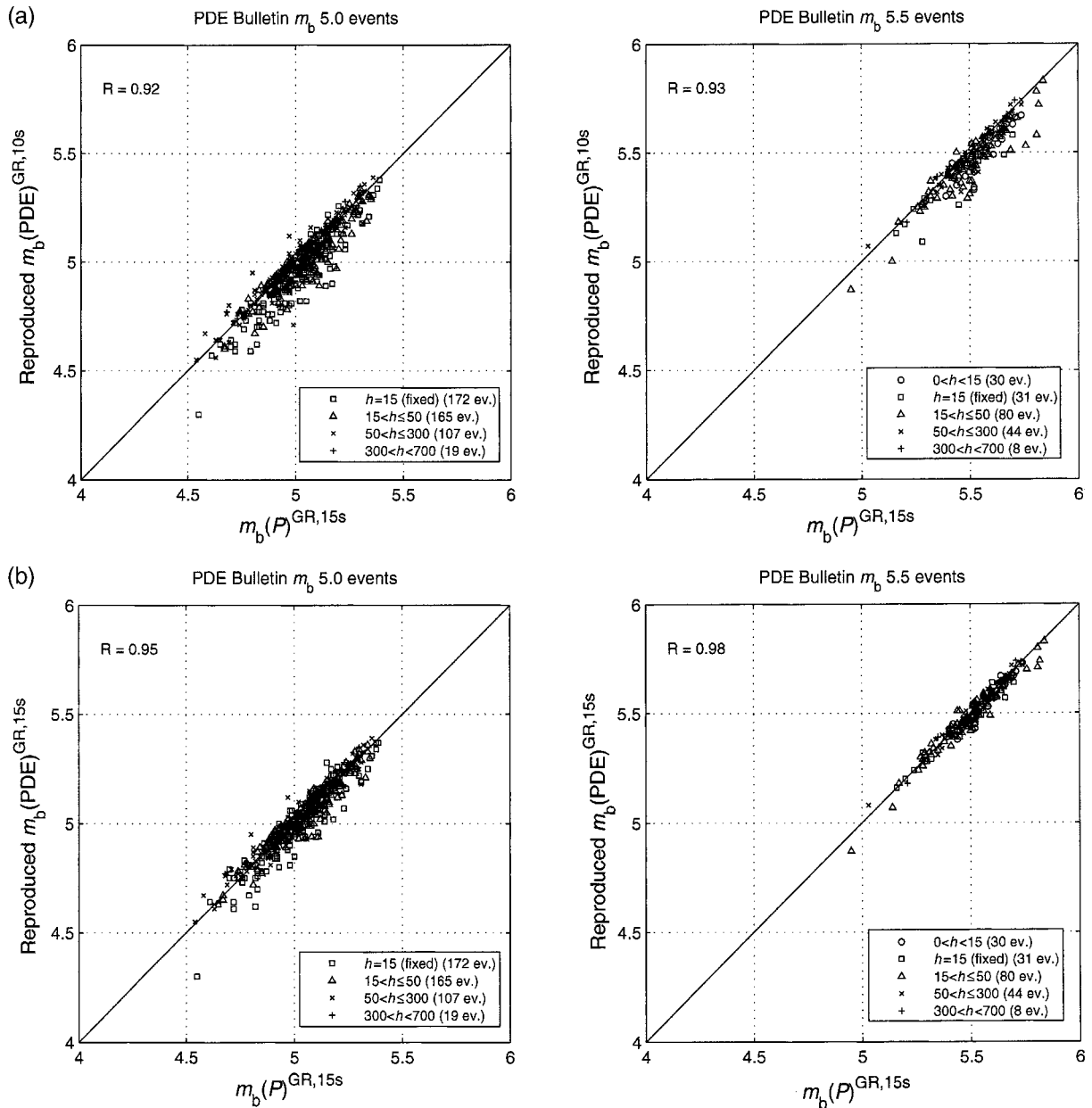


Figure 8. (a) Reproduced event  $m_b(\text{PDE})$  as a function of event  $m_b(P)$  for PDE bulletin  $m_b$  5.0 and 5.5 earthquakes. Reproduced PDE measurements are made using a time window length of 10 sec (to approximate the time window used in the PDE bulletin). Measurements of  $m_b(P)$  are made using a 15-sec time window and the distance and depth corrections for all magnitudes shown are Gutenberg–Richter (to match PDE bulletin). Correlation coefficient value ( $R$ ) is shown for each plot. (b) Reproduced event  $m_b(\text{PDE})$  as a function of event  $m_b(P)$  for PDE bulletin  $m_b$  5.0 and 5.5 earthquakes. Both magnitude types are measured using a 15-sec time window. Distance and depth corrections for all magnitudes shown are Gutenberg–Richter. Correlation coefficient value ( $R$ ) is shown for each plot. (E) Color versions of Figures 8a and 8b that include results for all six subsets of earthquakes [PDE bulletin  $m_b$  5.0 to 5.5] are available in the electronic edition of BSSA.)

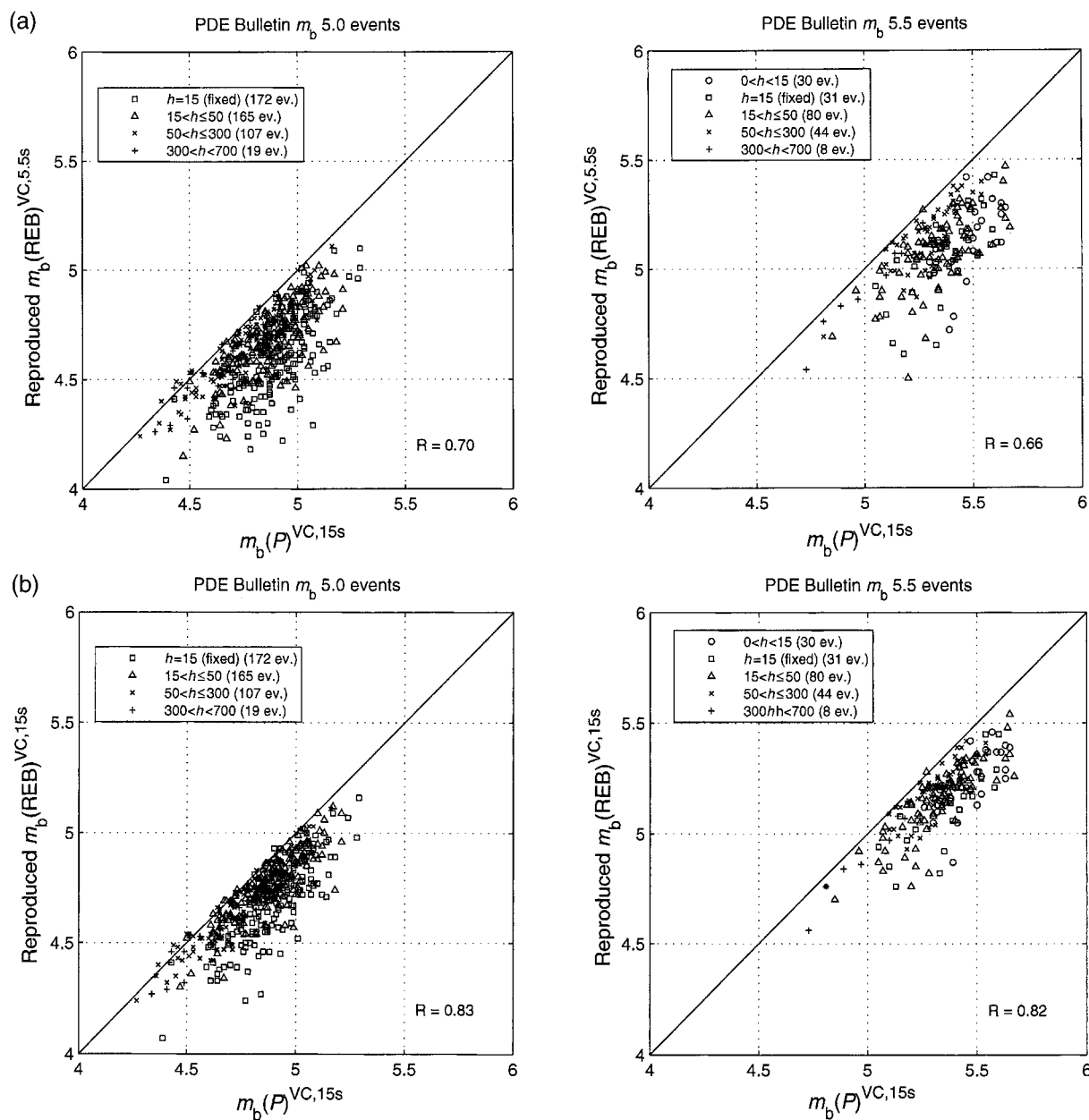


Figure 9. (a) Reproduced event  $m_b(\text{ReB})$  as a function of event  $m_b(P)$  for PDE bulletin  $m_b$  5.0 and 5.5 earthquakes. Reproduced ReB measurements are made using a time window length of 5.5 sec (to match the time window used in the ReB catalog). Measurements of  $m_b(P)$  are made using a 15-sec time window and the distance and depth corrections for all magnitudes shown are Veith–Clawson (to match ReB catalog). Correlation coefficient value ( $R$ ) is shown for each plot. (b) Reproduced event  $m_b(\text{ReB})$  as a function of event  $m_b(P)$  for PDE bulletin  $m_b$  5.0 and 5.5 earthquakes. Both magnitude types are measured using a 15-sec time window. Distance and depth corrections for all magnitudes shown are Veith–Clawson. Correlation coefficient value ( $R$ ) is shown for each plot. (E) A Color versions of Figures 9a and 9b that include results for all six subsets of earthquakes [PDE bulletin  $m_b$  5.0 to 5.5] are available in the electronic edition of BSSA.)

15 sec to match  $m_b(P)$  and eliminate any differences caused by different time window lengths. We find that  $m_b(\text{PDE})$  and  $m_b(P)$  are strongly correlated for the range of magnitudes and depths studied. When the magnitudes are compared using identical 15-sec time windows, the scatter is reduced (Fig. 8b); however, there exists a small offset between the two magnitudes, with  $m_b(P)$  being slightly larger on average.

We also analyze the relationship between  $m_b(\text{REB})$  and  $m_b(P)$ , using both a 5.5-sec time window length (Fig. 9a) and a window length of 15 sec (Fig. 9b) to measure  $m_b(\text{REB})$ . (© Color versions of these figures that include results for all six subsets of earthquakes [PDE bulletin  $m_b$  5.0 to 5.5] are available in the electronic version of BSSA.) Unlike the  $m_b(\text{PDE})-m_b(P)$  relationship, we find a strong depth dependence when  $m_b(\text{REB})$  is compared to  $m_b(P)$ . Since the PIDC displacement response is peaked at a frequency that is much higher than 1 Hz (Fig. 4), this response is not suitable for shallow earthquakes because high frequencies are too strongly attenuated. Although the USGS displacement response is also peaked at a frequency much higher than 1 Hz, magnitudes based on the USGS response are not as strongly affected as those based on the PIDC response because the responses are shaped differently and because the PIDC response has a peak around 3.4 Hz, whereas the USGS response peaks around 2.6 Hz. Because the PIDC displacement response causes strong attenuation of high frequencies,  $m_b(\text{REB})$  values are too low compared to traditional magnitudes, for shallow earthquakes. The scatter is reduced when equivalent time window lengths are used (Fig. 9b), although the  $m_b(\text{REB})-m_b(P)$  differences are still greater than the  $m_b(\text{PDE})-m_b(P)$  differences. We find that because of different time windows and response functions,  $m_b(P)$  is greater than  $m_b(\text{REB})$  for almost every event. The fact that differences between the magnitude scales decrease with increasing focal depth, independent of time window length, suggests that these differences should also decrease with decreasing source size as the dominant periods of  $P$  waves decrease. However, we expect that the events in this study are only slightly affected by this magnitude dependence since the range of magnitudes studied is narrow (i.e., PDE bulletin  $m_b$  5.0 to 5.5 events).

## Discussion

### Effect of Differing Seismic Networks on Event $m_b$

Though we have emphasized the differences in measurement procedures for different magnitude scales as they apply to station  $m_b$  values, a strong contributor to different values for published event  $m_b$  is the fact that the USGS, the PIDC, and the ISC all use different sets of stations when averaging station  $m_b$  values to obtain an event  $m_b$ . The USGS, for example, maintains a strong interest in tectonic areas such as the western United States and therefore receives more data from stations in those areas. Since stations in tectonic areas experience more attenuation than those in stable

continental regions, this leads to a network  $m_b$  that is biased low. An example of the differences that can result from using different networks of stations is shown in Figure 10, which compares the reproduced event  $m_b(\text{PDE})$  with the PDE bulletin event  $m_b$ , for all 2009 earthquakes in our dataset. The difference between the two event magnitudes is  $-0.024$  on average, with  $\sigma = 0.16$ . This average difference of  $-0.024$  magnitude units is similar to the  $-0.0171$  magnitude unit difference observed between the reproduced station  $m_b(\text{PDE})$  and published station  $m_b(\text{PDE})$  shown in Figure 5a. An important difference between Figures 5a and 10, however, is that Figure 5a compares station magnitudes whereas Figure 10 compares event magnitudes. Moreover, the two magnitudes compared in Figure 10 are based on different networks of stations (Fig. 2) and the 120 stations in this study that reported data to the USGS during 1996 to 1999 are only a subset of the complete USGS seismic network. Nevertheless, although the event magnitudes compared in Figure 10 are based on different networks, on average, there is only a  $-0.024$  magnitude unit difference between the magnitudes.

Because of discrepancies that can result from using different networks of stations to assign event  $m_b$ , we instead reproduce the procedures of the USGS and PIDC so that we can base our measurements on the same seismograms and focus on the different protocols. Thus, for each broadband seismogram we measure  $m_b(P)$ ,  $m_b(\text{PDE})$ , and  $m_b(\text{REB})$ . For a particular station, each of these magnitudes is computed using the same distance and depth information; therefore, only the amplitudes and periods (i.e.,  $\log(A/T)$  in equation [1]) are different.

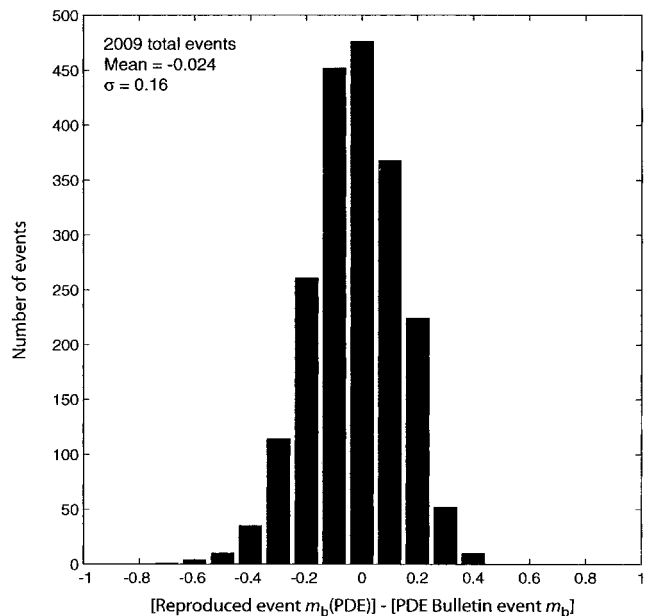


Figure 10. Histogram showing the distribution of offsets between reproduced PDE event  $m_b$  and PDE bulletin event  $m_b$  for all earthquakes in the dataset. Each bin represents a range of offsets with width 0.1 magnitude units.

Differences between  $m_b(P)$ ,  $m_b(\text{PDE})$ , and  $m_b(\text{REB})$

A summary of the differences we observe between  $m_b(P)^{\text{GR}}$ ,  $m_b(\text{PDE})^{\text{GR}}$ , and  $m_b(\text{REB})^{\text{GR}}$  is shown in Table 1. Events are separated according to depth and PDE bulletin magnitude. All body-wave magnitudes in Table 1 include Gutenberg–Richter distance and depth corrections (GR); therefore, any differences between the magnitudes result from different time window lengths and response functions. Although the magnitudes published in the REB use Veith–Clawson corrections for distance and depth (VC), in Table 1 we show  $m_b(\text{REB})$  using the Gutenberg–Richter correction terms (i.e.,  $m_b(\text{REB})^{\text{GR}}$ ), to be consistent with the other magnitude scales. By comparing the three magnitude scales using the same distance and depth correction terms, we are able to examine the effects of different time window lengths and response functions. We find that average  $m_b(P)^{\text{GR},15\text{s}}$  and average  $m_b(\text{PDE})^{\text{GR},10\text{s}}$  are similar to one another, suggesting that magnitudes based on the automated USGS procedure—

which has been used since 1991—are very similar to those based on simulated WWSSN short-period instruments with a slightly longer time window. Thus, we expect that magnitudes assigned from WWSSN short-period instruments during the 1970s and 1980s are consistent with those assigned by the automated procedure used since 1991 by the USGS, providing stability in  $m_b$  measurements over several decades. For  $m_b(\text{PDE})^{\text{GR}}$  values assigned using a time window length of 15 sec instead of 10 sec, the 15-sec window produces magnitudes that are only slightly larger than those based on a 10-sec window.

On the other hand, we find that for the  $m_b(\text{REB})^{\text{GR}}$  measurements the short window length of 5.5 sec often results in a lower magnitude for shallow events. Assigning  $m_b(\text{REB})^{\text{GR}}$  using the PIDC-defined time window length of 5.5 sec, instead of 15 sec, lowers  $m_b(\text{REB})^{\text{GR}}$  by an average of approximately 0.1 magnitude units for shallow events. In contrast, the deepest earthquakes show almost no depen-

Table 1  
Comparisons between  $m_b(P)$ , USGS PDE  $m_b$ , and PIDC REB  $m_b$

		Average Event $m_b$ (Using Gutenberg–Richter Distance and Depth Corrections) $\pm \sigma$						
	Depth (km)	No. of Events	$m_b(P)$ (tw*: 15 sec)	Reproduced PDE $m_b$ (tw: 10 sec)	Reproduced PDE $m_b$ (tw: 15 sec)	Reproduced REB $m_b$ (tw: 5.5 sec)	Reproduced REB $m_b$ (tw: 15 sec)	Harvard CMT $M_w$
PDE $m_b$ 5.0 Events	$h = 15$ (fixed) <sup>†</sup>	172	5.02 $\pm$ 0.15	4.96 $\pm$ 0.17	5.00 $\pm$ 0.16	4.72 $\pm$ 0.20	4.81 $\pm$ 0.18	5.38 $\pm$ 0.23
	$15 < h \leq 50$	165	5.07 $\pm$ 0.14	5.02 $\pm$ 0.15	5.06 $\pm$ 0.14	4.87 $\pm$ 0.16	4.95 $\pm$ 0.15	5.29 $\pm$ 0.21
	$50 < h \leq 300$	107	4.98 $\pm$ 0.18	4.98 $\pm$ 0.18	4.99 $\pm$ 0.17	4.87 $\pm$ 0.17	4.90 $\pm$ 0.17	5.25 $\pm$ 0.17
	$300 < h < 700$	19	5.05 $\pm$ 0.19	5.06 $\pm$ 0.19	5.06 $\pm$ 0.19	4.97 $\pm$ 0.19	4.97 $\pm$ 0.19	5.42 $\pm$ 0.18
PDE $m_b$ 5.1 Events	$0 < h < 15$	4	5.28 $\pm$ 0.21	5.19 $\pm$ 0.25	5.26 $\pm$ 0.21	4.90 $\pm$ 0.34	5.01 $\pm$ 0.26	5.90 $\pm$ 0.28
	$h = 15$ (fixed)	150	5.10 $\pm$ 0.15	5.04 $\pm$ 0.16	5.07 $\pm$ 0.15	4.81 $\pm$ 0.21	4.89 $\pm$ 0.19	5.40 $\pm$ 0.21
	$15 < h \leq 50$	161	5.14 $\pm$ 0.15	5.09 $\pm$ 0.15	5.13 $\pm$ 0.15	4.93 $\pm$ 0.17	5.01 $\pm$ 0.15	5.33 $\pm$ 0.20
	$50 < h \leq 300$	100	5.09 $\pm$ 0.16	5.09 $\pm$ 0.16	5.10 $\pm$ 0.16	4.97 $\pm$ 0.18	5.00 $\pm$ 0.18	5.30 $\pm$ 0.17
PDE $m_b$ 5.2 Events	$300 < h < 700$	27	5.09 $\pm$ 0.15	5.10 $\pm$ 0.16	5.10 $\pm$ 0.16	5.01 $\pm$ 0.16	5.02 $\pm$ 0.16	5.46 $\pm$ 0.16
	$0 < h < 15$	10	5.34 $\pm$ 0.13	5.27 $\pm$ 0.13	5.32 $\pm$ 0.15	5.01 $\pm$ 0.20	5.14 $\pm$ 0.16	5.80 $\pm$ 0.24
	$h = 15$ (fixed)	99	5.22 $\pm$ 0.16	5.17 $\pm$ 0.17	5.20 $\pm$ 0.17	4.91 $\pm$ 0.21	5.01 $\pm$ 0.19	5.45 $\pm$ 0.22
	$15 < h \leq 50$	145	5.22 $\pm$ 0.14	5.18 $\pm$ 0.14	5.22 $\pm$ 0.14	5.02 $\pm$ 0.17	5.10 $\pm$ 0.15	5.39 $\pm$ 0.22
PDE $m_b$ 5.3 Events	$50 < h \leq 300$	98	5.18 $\pm$ 0.17	5.17 $\pm$ 0.17	5.18 $\pm$ 0.17	5.07 $\pm$ 0.17	5.09 $\pm$ 0.17	5.36 $\pm$ 0.20
	$300 < h < 700$	12	5.22 $\pm$ 0.09	5.23 $\pm$ 0.09	5.23 $\pm$ 0.09	5.12 $\pm$ 0.10	5.13 $\pm$ 0.11	5.58 $\pm$ 0.19
	$0 < h < 15$	13	5.38 $\pm$ 0.18	5.33 $\pm$ 0.19	5.37 $\pm$ 0.18	5.05 $\pm$ 0.24	5.17 $\pm$ 0.22	5.72 $\pm$ 0.23
	$h = 15$ (fixed)	77	5.28 $\pm$ 0.15	5.21 $\pm$ 0.17	5.25 $\pm$ 0.15	4.95 $\pm$ 0.22	5.05 $\pm$ 0.20	5.54 $\pm$ 0.23
PDE $m_b$ 5.4 Events	$15 < h \leq 50$	137	5.32 $\pm$ 0.14	5.27 $\pm$ 0.15	5.31 $\pm$ 0.14	5.09 $\pm$ 0.17	5.18 $\pm$ 0.16	5.52 $\pm$ 0.27
	$50 < h \leq 300$	81	5.29 $\pm$ 0.16	5.29 $\pm$ 0.15	5.30 $\pm$ 0.15	5.16 $\pm$ 0.17	5.19 $\pm$ 0.17	5.40 $\pm$ 0.22
	$300 < h < 700$	14	5.38 $\pm$ 0.15	5.41 $\pm$ 0.14	5.41 $\pm$ 0.14	5.33 $\pm$ 0.14	5.33 $\pm$ 0.14	5.65 $\pm$ 0.25
	$0 < h < 15$	28	5.45 $\pm$ 0.14	5.40 $\pm$ 0.17	5.43 $\pm$ 0.14	5.10 $\pm$ 0.21	5.21 $\pm$ 0.18	5.88 $\pm$ 0.26
PDE $m_b$ 5.5 Events	$h = 15$ (fixed)	49	5.40 $\pm$ 0.15	5.34 $\pm$ 0.17	5.38 $\pm$ 0.16	5.06 $\pm$ 0.22	5.17 $\pm$ 0.20	5.60 $\pm$ 0.28
	$15 < h \leq 50$	83	5.42 $\pm$ 0.13	5.37 $\pm$ 0.13	5.41 $\pm$ 0.12	5.19 $\pm$ 0.15	5.27 $\pm$ 0.13	5.61 $\pm$ 0.27
	$50 < h \leq 300$	55	5.33 $\pm$ 0.15	5.31 $\pm$ 0.16	5.32 $\pm$ 0.16	5.20 $\pm$ 0.16	5.22 $\pm$ 0.15	5.47 $\pm$ 0.23
	$300 < h < 700$	10	5.41 $\pm$ 0.14	5.42 $\pm$ 0.14	5.42 $\pm$ 0.14	5.34 $\pm$ 0.13	5.35 $\pm$ 0.14	5.73 $\pm$ 0.24
PDE $m_b$ 5.5 Events	$0 < h < 15$	30	5.55 $\pm$ 0.11	5.49 $\pm$ 0.12	5.53 $\pm$ 0.11	5.21 $\pm$ 0.16	5.32 $\pm$ 0.12	5.76 $\pm$ 0.24
	$h = 15$ (fixed)	31	5.48 $\pm$ 0.14	5.43 $\pm$ 0.14	5.45 $\pm$ 0.13	5.16 $\pm$ 0.19	5.25 $\pm$ 0.17	5.66 $\pm$ 0.27
	$15 < h \leq 50$	80	5.50 $\pm$ 0.16	5.45 $\pm$ 0.15	5.49 $\pm$ 0.16	5.25 $\pm$ 0.18	5.33 $\pm$ 0.17	5.75 $\pm$ 0.27
	$50 < h \leq 300$	44	5.52 $\pm$ 0.13	5.51 $\pm$ 0.14	5.52 $\pm$ 0.13	5.39 $\pm$ 0.16	5.42 $\pm$ 0.14	5.64 $\pm$ 0.25
	$300 < h < 700$	8	5.48 $\pm$ 0.16	5.48 $\pm$ 0.17	5.49 $\pm$ 0.17	5.38 $\pm$ 0.18	5.39 $\pm$ 0.18	5.88 $\pm$ 0.28

\*Length of time window used to make the measurements, beginning at the  $P$ -wave arrival time.

<sup>†</sup>No PDE  $m_b$  5.0 events with a focal depth less than 15 km are present in our dataset.

dence on time window length. This result applies to both  $m_b(\text{PDE})^{\text{GR}}$  and  $m_b(\text{REB})^{\text{GR}}$ , indicating that the length of the time window used to measure amplitude matters only for shallow earthquakes, where the depth phases ( $pP$  and  $sP$ ) are often the largest arrivals. Regardless of time window length, however,  $m_b(\text{REB})^{\text{GR}}$  is substantially lower than  $m_b(P)^{\text{GR}}$  for shallow earthquakes because of differences between the PIDC displacement response and WWSSN displacement response (Fig. 4). The PIDC response, which is peaked at a much higher frequency than the WWSSN response, is not suitable for shallow earthquakes because the dominant frequencies in the radiated signal are often strongly attenuated. Although the USGS displacement response is also peaked at a frequency much higher than the WWSSN response, magnitudes based on the USGS response are not as strongly affected as those based on the PIDC response since the PIDC response is peaked at a significantly higher frequency than the USGS response (3.4 Hz vs. 2.6 Hz).

Moment magnitudes from Harvard CMTs are also given in Table 1 and are found to be greater on average than all of the body-wave magnitudes. (Ⓔ A discussion of the relationship among  $m_b(P)$ ,  $M_w$ , and  $M_s$  for the events studied is available in the electronic edition of BSSA.)

#### Summary of Factors Contributing to Differences Between the $m_b$ Scales

In Table 2, we give a summary of the factors contributing to the observed differences between the  $m_b$  scales studied. When equivalent 15-sec time windows are used, the average difference between  $m_b(P)^{\text{GR}}$  and  $m_b(\text{PDE})^{\text{GR}}$  is close to zero for all depth ranges. On the other hand, if  $m_b(\text{PDE})^{\text{GR}}$  is measured using a time window length of 10 sec, a discrepancy does exist between  $m_b(P)^{\text{GR}}$  and  $m_b(\text{PDE})^{\text{GR}}$  for shallow earthquakes ( $h \leq 50$  km). In this case, the shorter 10 sec window misses some of the larger depth phase arrivals, causing the amplitudes to be underestimated; thus,  $m_b(P)^{\text{GR},15\text{s}}$  sec will exceed  $m_b(\text{PDE})^{\text{GR},10\text{s}}$  sec by 0.05 to 0.06 magnitude units.

For earthquakes with focal depths of 15 km or less, the average  $m_b(P)^{\text{GR}}$  is 0.22 to 0.23 magnitude units greater than  $m_b(\text{REB})^{\text{GR}}$  when equivalent 15-sec time windows are used. If  $m_b(\text{REB})^{\text{GR}}$  is measured using the PIDC-defined window length of 5.5 sec, however, then the  $m_b(\text{REB})^{\text{GR}}$  value will be lowered by an additional 0.10 to 0.11 magnitude units (when  $h \leq 15$  km). While the choice of time window—either 5.5 sec or 15 sec—for the REB magnitudes has almost no effect for the deepest earthquakes ( $h > 300$  km), an average difference of 0.07 magnitude units exists between  $m_b(P)^{\text{GR},15\text{s}}$  and  $m_b(\text{REB})^{\text{GR},15\text{s}}$  for deep events because of differences between the PIDC and WWSSN responses.

Although the difference between  $m_b(P)$  and  $m_b(\text{REB})$  is smallest for deep earthquakes, a large discrepancy between REB and PDE bulletin magnitudes exists for earthquakes at all depths (Murphy *et al.*, 2001). This is because the PIDC and USGS use different corrections for distance and depth (Veith–Clawson and Gutenberg–Richter, respectively) when assigning  $m_b$ . The Gutenberg–Richter corrections are greater for all depths and become increasingly greater than the Veith–Clawson corrections as depth increases. We find that the Gutenberg–Richter corrections are an average of 0.42 magnitude units higher for the deepest earthquakes ( $h > 300$  km). This large observed difference between the Veith–Clawson and Gutenberg–Richter corrections for deep earthquakes agrees with Murphy and McLaughlin (1998), who found that the difference between the two corrections can exceed 0.6 magnitude units for earthquakes in the 600- to 700-km-depth range. Thus, a large offset exists between published REB and PDE magnitudes for deep earthquakes even though the attenuating effects of the PIDC filter are minimal. Differences between published REB and PDE magnitudes for shallow earthquakes result primarily from the different responses, whereas for deep earthquakes the differences are primarily the result of different corrections for distance and depth.

The average period for all station observations, when measured in 15-sec time windows, is 0.99 sec for the simulated WWSSN SP signals, 0.86 sec for the reproduced PDE waveforms, and 0.80 sec for the simulated REB records. Since these periods are all measured using the same time

Table 2  
Differences in  $m_b$  Resulting from Different Time Window Lengths, Responses, and Corrections for Distance and Depth, as a Function of Depth (PDE Bulletin  $m_b$  5.0–5.5 events)

Depth (km)	Average Difference between Event $m_b$ Values				
	$[m_b(P)^{\text{GR},15\text{s}}] - [m_b(\text{PDE})^{\text{GR},10\text{s}}]$	$[m_b(P)^{\text{GR},15\text{s}}] - [m_b(\text{PDE})^{\text{GR},15\text{s}}]$	$[m_b(P)^{\text{GR},15\text{s}}] - [m_b(\text{REB})^{\text{GR},5.5\text{s}}]$	$[m_b(P)^{\text{GR},15\text{s}}] - [m_b(\text{REB})^{\text{GR},15\text{s}}]$	[Average $B^{\text{GR}}] - [\text{Average } B^{\text{VC}}]$
$0 < h < 15$	0.06	0.02	0.34	0.23	0.09
$h = 15$ (fixed)	0.06	0.02	0.31	0.22	0.12
$15 < h \leq 50$	0.05	0.01	0.20	0.13	0.18
$50 < h \leq 300$	0.01	0.00	0.12	0.09	0.24
$300 < h < 700$	−0.01	−0.01	0.08	0.07	0.42

$B^{\text{GR}}$ , correction for distance and depth based on Gutenberg and Richter (1956);  $B^{\text{VC}}$ , correction for distance and depth based on Veith and Clawson (1972).

window length, the differences between them are mainly the result of different response functions (Fig. 4) and differences in the type of signal from which the period is measured (i.e., WWSSN waveforms are simulated from displacement signals; PDE and REB records are simulated from velocity seismograms). Since the average periods of the PDE and REB records differ by only 0.06 sec the differences between the two for a fixed time window are also due in part to a dependence on source corner frequency. This is only a slight effect, however, and not as big as the factors we address in this study since the range of magnitudes studied is narrow (i.e., PDE bulletin  $m_b$  5.0 to 5.5 events). Because the average reproduced PDE and REB periods are less than 1.0 secs this will increase the  $\log(A/T)$  portion of the  $m_b$  calculation relative to WWSSN signals with periods near 1.0 sec. Reproduced PDE and REB records have periods much less than 1.0 sec because of the high-frequency passbands of the USGS and PIDC responses and because the periods are measured from velocity seismograms.

### Conclusions

We obtain body-wave magnitude ( $m_b$ ) measurements for 2009 earthquakes from 1996 to 1999 listed in the PDE bulletin having  $m_b$  between 5.0 to 5.5 and that also have moment tensor solutions available from the Harvard CMT catalog. A total of 31,280 broadband seismograms are analyzed for an average of 15 stations per event. The seismic stations recording the largest number of earthquakes are located predominantly on the Eurasian continent. For each broadband seismogram studied, three different types of magnitude are assigned:  $m_b(\text{PDE})$ ,  $m_b(\text{REB})$ , and  $m_b(P)$ . We reproduce both the automated protocol followed by the USGS to assign body-wave magnitude,  $m_b(\text{PDE})$ , and the automated procedure used by the PIDC to assign magnitude,  $m_b(\text{REB})$ . By reproducing the automated procedures of these agencies, we can base our measurements on the same seismograms and eliminate the discrepancies that result from using different networks of stations. Since neither the PDE nor the REB magnitude scale is based on a specific instrument, we compare the reproduced PDE and REB magnitudes to a traditional magnitude measurement,  $m_b(P)$ , that is based on the Worldwide Standard Seismographic Network (WWSSN) short-period instrument, used for about 20 years before digital instruments became widely available. The traditional method ( $m_b(P)$ ) is based on displacement measurements, whereas the PDE and REB measurements are based on velocity signals.

Differences between  $m_b(\text{PDE})$ ,  $m_b(\text{REB})$ , and  $m_b(P)$  arise from four factors: response function, time window length, corrections for hypocentral depth, and corrections for epicentral distance. We find that  $m_b(\text{PDE})$  and  $m_b(P)$  are strongly correlated for the range of magnitudes and depths studied, with  $m_b(P)$  being larger by an average of 0.04 magnitude units, when  $m_b(\text{PDE})$  is measured using a 10-sec time

window. The PDE window length of 10 sec when compared to a traditional window length of 15 sec, has only a minor effect on  $m_b(\text{PDE})$ . When equivalent 15-sec, time windows are used, magnitudes based on WWSSN short-period instruments are very similar to those based on the automated procedure used since 1991 by the USGS.

In contrast to the similarity between  $m_b(\text{PDE})$  and  $m_b(P)$ , we find a strong dependence on depth, response function, and time window length when  $m_b(\text{REB})$  is compared to  $m_b(P)$ . Because the PIDC displacement response is peaked at a much higher frequency ( $\sim 3.4$  Hz) than either the USGS ( $\sim 2.6$  Hz) or WWSSN response ( $\sim 1.6$  Hz), magnitudes based on the PIDC procedure (i.e.,  $m_b(\text{REB})$ ) are too small for shallow earthquakes. The high-frequency passband of the PIDC response causes the short-period portion of the signal to be attenuated too strongly, compared to a traditional measurement. The observed differences between REB and PDE bulletin magnitudes for shallow earthquakes result primarily from the different response functions whereas for deep earthquakes the differences are primarily the result of different corrections for distance and depth. For consistency with  $m_b(P)$  and  $m_b(\text{PDE})$ , the PIDC could produce a classical  $m_b$  measurement in addition to its current  $m_b(\text{REB})$ , styled after either the  $m_b(P)$  or  $m_b(\text{PDE})$  procedure. This classical measurement would be a very useful and important source parameter since it would be based on a fixed network of stations and would be consistent with magnitudes measured using WWSSN short-period instruments. We also recommend that the PIDC continue to assign magnitudes using its current procedure since the PIDC  $m_b$ , being a higher frequency measurement, may work better than a traditionally measured magnitude such as  $m_b(P)$  for purposes of applying the  $m_b-M_s$  discriminant.

Since PDE bulletin magnitudes are based on Gutenberg–Richter distance and depth corrections, whereas published REB magnitudes are based on Veith–Clawson corrections, using different correction terms causes additional differences between the two magnitudes. The Gutenberg–Richter corrections are greater for all depths and become increasingly greater than the Veith–Clawson corrections as depth increases. The deepest earthquakes show an average separation of 0.4 magnitude units between the Gutenberg–Richter and Veith–Clawson correction terms.

### Acknowledgments

We would like to thank Jack Murphy and an anonymous reviewer for their helpful reviews of the manuscript. We benefited greatly from comments by Ray Buland, Jim Dewey, and Scott Phillips. Data were retrieved from the Incorporated Research Institutions in Seismology (IRIS), Data Management Center in Seattle, Washington. The Generic Mapping Tools (GMT) software package of Wessel and Smith (1998) was used to make Figures 1 and 2. This research was sponsored partly by the Defense Threat Reduction Agency under Contract DTRA01-00-C-0074 and DTRA01-00-C-0031 and also partly by the Department of Earth and Environmental Sciences, Columbia University. This is Lamont-Doherty Earth Observatory Contribution Number 6808.

## References

- Centroid Moment Tensor (CMT) Catalog, [www.seismology.harvard.edu/CMTsearch.html](http://www.seismology.harvard.edu/CMTsearch.html).
- Dewey, J. W. (1999). On the PIDC/USGS  $m_b$  discrepancy, *Seism. Res. Lett.* **70**, 211–212, (abstract).
- Granville, J. P., W.-Y. Kim, and P. G. Richards (2002). An assessment of seismic body-wave magnitudes published by the Prototype International Data Centre, *Seism. Res. Lett.* **73**, 893–906.
- Gutenberg, B., and C. F. Richter (1956). Magnitude and energy of earthquakes, *Annali di Geofisica* **9**, 1–15.
- International Data Centre (1999). *IDC Processing of Seismic, Hydroacoustic, and Infrasonic Data*, Version 5.2.1, 233–255.
- Luh, P. C. (1977). A scheme for expressing instrumental responses parametrically, *Bull. Seism. Soc. Am.* **67**, 957–969.
- Murphy, J. R., and B. W. Barker (1996). An evaluation of the IDC/NEIS  $m_b$  anomaly, Technical Memorandum to NTPO/OSD, Maxwell/S-Cubed, September.
- Murphy, J. R., and K. L. McLaughlin (1998). Comment on “Empirical determination of depth-distance corrections for  $m_b$  and  $M_w$  from Global Seismograph Network stations” by Guust Nolet, Steve Krueger, and Robert M. Clouser, *Geophys. Res. Lett.* **25**, 4269–4270.
- Murphy, J. R., J. L. Stevens, T. J. Bennett, B. W. Barker, and M. E. Marshall (2001). Development of improved seismic magnitude measures for use at the International Data Center, final technical report, 135 pp.
- Murphy, J. R., and B. W. Barker (2003). Revised distance and depth corrections for use in the estimation of short-period  $P$ -wave magnitudes, *Bull. Seism. Soc. Am.* **93**, 1746–1764.
- Richter, C. F. (1935). An instrumental magnitude scale, *Bull. Seism. Soc. Am.* **25**, 1–32.
- Veith, K. F., and G. E. Clawson (1972). Magnitude from short-period  $P$ -wave data, *Bull. Seism. Soc. Am.* **62**, 435–452.
- Wessel, P., and W. H. F. Smith (1998). New, improved version of Generic Mapping Tools released, *EOS Trans. Am. Geophys. Union* **79**, 579.
- Willemann, R. J. (1998). Network amplitude biases in the ISC bulletin, *EOS Trans. Am. Geophys. Union* **79**, 588 (abstract).
- Willmore, P. L. (1979). *Manual of Seismological Observatory Practice*, Report SE-20, WDC-A for Solid Earth Geophysics, U.S. Dept. of Commerce, National Oceanic and Atmospheric Administration, Boulder, Colorado.

Lamont-Doherty Earth Observatory of Columbia University  
 61 Route 9W  
 Palisades, New York 10964  
 johng@ldeo.columbia.edu  
 richards@ldeo.columbia.edu  
 wykim@ldeo.columbia.edu  
 sykes@ldeo.columbia.edu

Manuscript received 13 August 2004.